A Compact, Air-Cooled Zeeman Slower As A Cold Atom Source

by

Ingrid Kaldre

Department of Physics
Duke University

Date:_____

Approved:

_____
Dr. John E. Thomas, Supervisor

_____
Dr. Daniel J. Gauthier

_____
Dr. M. Ronen Plesser

A thesis submitted in partial fulfillment of the requirements
for graduation with distinction in physics in the
Department of Physics at Trinity College,
Duke University

2006

<u>ABSTRACT</u>

(Physics)

A Compact, Air-Cooled Zeeman Slower As A Cold Atom Source

by

Ingrid Kaldre

Department of Physics
Duke University

Date:_____

Approved:

_____

Dr. John E. Thomas, Supervisor

_____

Dr. Daniel J. Gauthier

_____

Dr. M. Ronen Plesser

A thesis submitted in partial fulfillment of the requirements
for graduation with distinction in physics in the
Department of Physics at Trinity College,
Duke University

2006

Abstract

This thesis outlines the preliminary construction of an improved experimental apparatus dedicated to the investigation of ultra-cold fermions. Our research aims to discover the new physics in the interaction between fermions, the fundamental building blocks of all matter. The central component of this project is the design, construction and testing of a more compact and efficient slowing apparatus, the Zeeman Slower. This multi-coil solenoid allows us to slow ^{6}Li atoms from 1500 m/s to 20 m/s at which point the Fermi gas is trapped and studied.

The improved slower is 30 cm long, utilizes only two power supplies and does not require water-cooling. It is more compact and has proven simpler to construct and maintain than the previous slower design and is capable of slowing an adequate number of atoms for our experiment. This document describes the motivation for the new design, as well as the construction and testing of the improved slowing apparatus.

Acknowledgments

After four years at the JET lab, I have learned one important lesson: always resist the urge to wear a skirt and heels to work. Inevitably on days you dress up, you will find yourself fixing lab equipment seven feet off the ground, lugging around dusty power supplies, and machining parts on a greasy lathe. As I transition into the stuffy world of business suits, I will miss the dirt and grime of the lab, I will miss that one glorious moment of discovery, and I will certainly miss all of you.

John, thank you for taking a chance on a lowly freshman. You have been an attentive teacher and counselor, a constant source of encouragement and laughs. A genuine affection and concern for your students is apparent in everything you do. Your vitality is certainly the source of your success. Try not to get hit by lightening!

A thank you to Staci Hemmer and Mike Gehm for their vast wisdom and patience. A special thanks to Mike for never running out of reasons to bet me a dollar - I did almost finish that 1 lb. block of cheddar cheese. For the perfect "Ah-nold" impersonation, for tolerating my never ending barrage of questions, a heartfelt thanks to Joe Kinast. Thank you for the conversation. To Le Luo and Bason Clancy for the summer we made it work! To Andrey for his Estonian jokes, and to James for always managing to steal my computer space when I needed it.

To my high school Physics teacher, Dr. Makous, I owe it all to you. Your love of Physics is contagious. You gave me the confidence to pursue my curiosity. You taught me the importance of believing in myself.

And finally to DJ Cecile, my instructor and my friend. Thank you for your time and your patience. Thank you for the jokes to get me through those dark days and nights of problems sets. Your generosity has been overwhelming. Your friendship means the world to me.

N, I will never forget

Contents

List of Figures

List of Tables

Chapter 1

Introduction

1.1 Overview

Our group is currently conducting experiments which investigate the behavior of fermions, the fundamental building blocks of all matter. To ultimately study interactions in an ultracold Fermi gas, our objective is to more efficiently trap and cool neutral ^{6}Li atoms utilizing the mechanical properties of light.

1.2 Historical Background

The foundation for our work dates back to the 17th century. In 1619, Johannes Kepler observed that dust particles in the wake of a comet are pushed by light pressure, causing the tails to always point away from the sun [1]. This insight into light's mechanical properties remained overlooked for hundreds of years, until the 20th century when researchers began to understand and devise a means to harness light's mechanical power.

The first substantial analysis of light pressure appeared in 1917. In his monumental paper, "On the Quantum Theory of Radiation," Einstein analyzed the momentum transfer between atoms and photons as the latter are absorbed and

spontaneously emitted [2]. Forty years later, Einstein's work found a practical application in the invention of the laser, and in the following decades, in the field of cooling and trapping.

Researchers became interested in cooling atoms for the advantages slow atoms present. Slow atoms have longer observation times making their properties easier to measure. Furthermore, only at small momentum and a large de Broglie wavelength is the quantum nature of a particle discernible. In 1975, two groups independently introduced the idea of laser cooling - slowing atoms using light radiation. Their proposal finally came to fruition in 1985 with William Phillips' invention of the Zeeman Slower - a series of electromagnets, which maintain atoms in constant resonance with an incoming laser beam [3]. The Zeeman Slower has become a common tool in atomic, molecular and optical physics to slow atoms before they can be trapped and studied.

1.3   Subject of Inquiry

1.3.1   Degenerate Fermi Gas

Of the two distinct sets of particles in nature, bosons and fermions, the latter comprise the focus of our investigations. Fermions, such as electrons, protons and quarks, are distinguished by a half-integral spin. Quantum mechanics sets strict occupancy rules for these particles, restricting a specific quantum state to one or no fermions [4].

When a Fermi gas is cooled near absolute zero, fermions fill quantum states beginning in a state of lowest energy and stacking sequentially to a state of highest energy, the Fermi energy. The gas is deemed degenerate in this configuration. It

is interactions in a degenerate Fermi gas, which attracts our interest. Through this particular system, we can model many interesting physical systems like superconductors and neutron stars [5].

1.3.2 Atomic Fermions

In our lab, we study ^{6}Li, an isotope of the more prevalent ^{7}Li, which behaves as a composite fermion. Angular momentum addition rules establish a net half-integral spin for atoms with odd numbers of fermions, the electrons, protons and neutrons which comprise the atom. ^{6}Li is composed of nine fermions and behaves as a fermion. Atomic fermions prove much easier to study than electrons and protons due to enhanced control over the system.

1.4 Experimental Set-Up

In order to trap a degenerate ^{6}Li gas and then study its interactions, we must first slow and cool the atoms. ^{6}Li is first heated in an oven to 700 K, transforming it from the solid to the gas state. The atoms, now traveling at an average velocity of 1500 m/s, enter the Zeeman Slower in a collimated stream. They are laser cooled to speeds below 100 m/s. Only the coldest atoms, averaging 20 m/s, can then be captured in the six crossbeams of the Magneto Optical Trap (MOT). Figure 2.2 displays our experimental set-up.

1.5 Motivations for Current Work

Our group is currently developing a new atom cooling and trapping apparatus, which is more compact than the previous design and utilizes knowledge we have

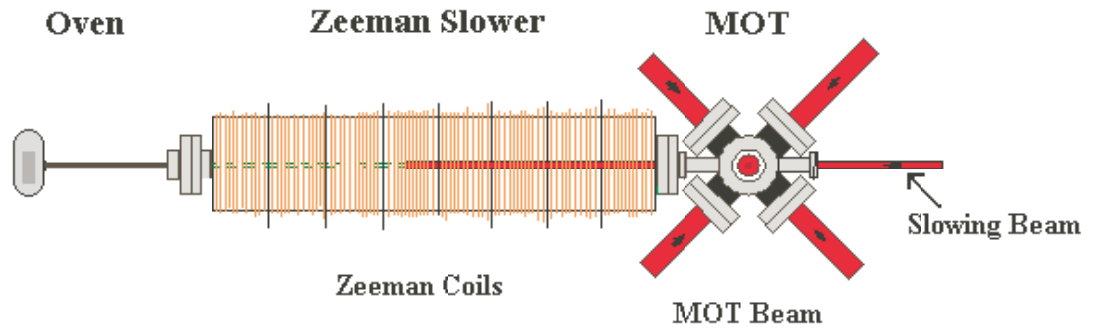**Figure 1.1**: Our set-up from the oven to the MOT.

gained in a decade of experiments. For details on the old design see the following dissertations: Ken O'Hara [6] and Mike Gehm [7]. A key component in the redesign is a simplification of the atomic source and slowing region. Our goal was to design a compact, air-cooled, and cost effective Zeeman Slower to further our study of atomic fermions.

Chapter 2

Zeeman Cooling

2.1   Laser Cooling

In order to capture and study a ^{6}Li gas, our atoms must first be significantly slowed
down. The most efficient way of slowing atoms is with laser cooling. In this process,
a stream of photons interact with an atom. As long as a laser beam is resonant
with an atomic transition frequency, the atom will absorb an incoming photon
and at a later time expel the photon in an arbitrary direction. When assailed by
many photons, an atom emits photons in random directions. Consequently, the net
momentum change resulting from photon emission is equal to zero. On the other
hand, the net momentum change resulting from photon absorption is consistently
in the direction opposing the atom's forward trajectory. If we bombard an atom
with photons that carry momentum $p = h/\lambda$, where h is Planck's constant and λ
is the wavelength of the light, the atom will experience a velocity change

$$\Delta v = \frac{h}{m\lambda},\tag{2.1}$$

where $m = 9.99 \times 10^{-27}$ kg [7] is the mass of the atom. Figure 2.2 illustrates the
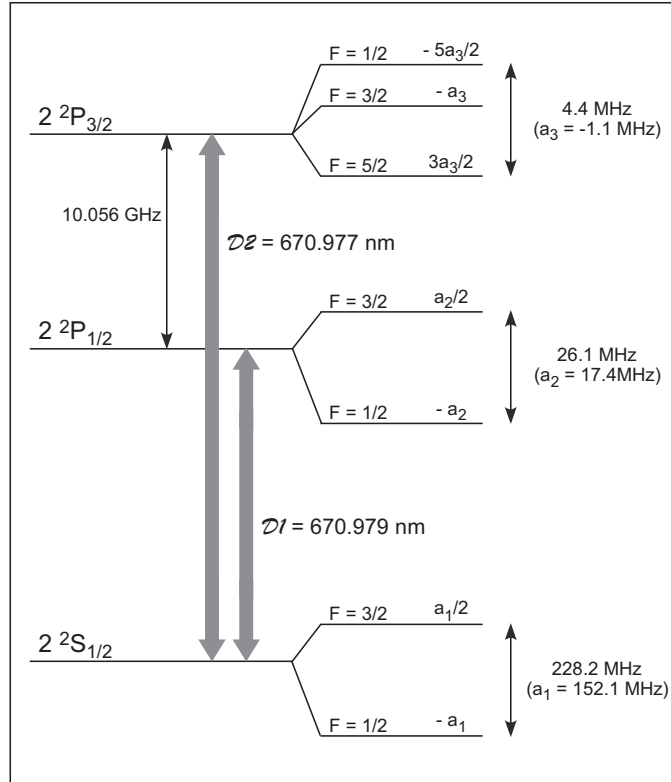absorption and emission process.

Figure 2.1: A level diagram for the ground and 2P states of ^{6}Li. We slow atoms using the D2 transition [7]

.

In our experiment, we choose the slowing transition

$$2S_{1/2}(F = 3/2, M_F = 3/2) \rightarrow 2P_{3/2}(F' = 5/2, M_{F'} = 5/2). \qquad (2.2)$$

for ^{6}Li, where F is the total angular momentum and M_F is the spin projection. For a level diagram illustrating this transition, see Figure 2.1. Assailed by photons of wavelength, $\lambda = 671$ nm, our atoms will experience a velocity change, $\Delta v = 10$ cm/s per photon. In order for a ^{6}Li atom traveling at an average velocity of 1.5×10^5 cm/s to come to rest, the atom must absorb and emit a photon about 1.5×10^4 times. Lithium 6 emits a photon about every 27 ns, so a ^{6}Li atom traveling at 1.5×10^5
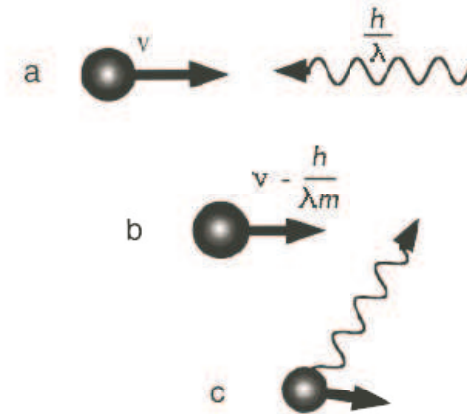
Figure 2.2: (a) An atom with velocity v encounters a photon with momentum h/λ; (b) after absorbing the photon, the atoms is slowed by $h/m\lambda$; (c) after re-radiation in a random direction, on average the atom is slower than in (a) [3].

cm/s will come to rest in 0.4 ms as long as it is bombarded by resonant photons.

2.2   Doppler Shift

In an ideal world a laser beam, tuned to a transition frequency, would suitably slow atoms. In reality, as an atom and a photon move toward one another, the atom experiences a blue shifted photon - the photon appears to have a higher frequency than if it were standing still. The Doppler shift will only interfere with slowing atoms if it is large in comparison with the resonance width. In our case, with $v = 1500$ m/s and $\lambda = 671$ nm,

$$\Delta\nu_{\text{Doppler}} = v/\lambda \tag{2.3}$$

$$\approx 2\,\text{GHz}$$

while with $\tau_{\text{Spont}} = 27$ ns,

$$\Delta\nu_{\text{Spont}} = \frac{1}{2\pi\tau_{\text{Spont}}} \qquad (2.4)$$

$$\approx 5.7\,\text{MHz}$$

The Doppler shift is much greater than the resonance width and must be accounted for in order to slow atoms.

To keep photons in resonance with an atom, we must lower the frequency of our laser by

$$\Delta\omega = \frac{2\pi v}{\lambda}. \qquad (2.5)$$

Further, an atom's velocity relative to the photon beam will change as it is slowed down. This velocity change throws our chosen laser frequency off resonance with the atom's slowing transition. In order to slow many atoms, we must continually account for this velocity-dependent Doppler shift.

Two methods have been developed to keep photons continuously in resonance with an atomic beam. The first, chirp cooling, continually tunes a laser beam to account for the changing Doppler shift. This method produces a pulse of slow atoms. The second, Zeeman cooling, utilizes a spatially varying magnetic field to shift the energy levels of an atom, changing the atomic transition frequency during the entirety of an atom's forward trajectory [8]. We choose the latter method because it produces a steady stream of slow atoms.

In the case of an atomic beam, where atoms have a wide range of velocities, Zeeman cooling slows a set of atoms into a narrow velocity range. Atoms traveling at the velocity for which we calculate the magnetic field taper will continually absorb photons and decelerate. Atoms traveling the length of the slower faster and

slower than this velocity will absorb and decelerate very little until they come into resonance with the beam [3]. Thus the slowing beam will grab atoms with a wide spread of velocities at different times during their trajectory, slowing all atoms from a maximum velocity down to zero.

2.3 Zeeman Effect

We Zeeman shift our ^{6}Li atoms to keep them constantly in resonance with incoming photons. In the presence of a magnetic field, a ^{6}Li atom experiences the perturbation

$$H' = -(\vec{\mu_L} \cdot \vec{B} + \vec{\mu_S} \cdot \vec{B}), \tag{2.6}$$

In this perturbation, the orbital and spin components of the atom's magnetic dipole moment are:

$$\vec{\mu_L} = -\frac{e\vec{L}}{2m_e} \tag{2.7}$$

$$\vec{\mu_S} = -\frac{e\vec{S}}{m_e}. \tag{2.8}$$

with $\vec{L}$ the orbital angular momentum, $\vec{S}$ the spin angular momentum and $\vec{B}$ the magnetic field. Now substituting Equations (2.7) and (2.8) into (2.6) yields

$$H' = \frac{e\hbar}{2m_e}\left(\frac{\vec{L}}{\hbar} + \frac{2\vec{S}}{\hbar}\right) \cdot \vec{B} \tag{2.9}$$

A generalized form of the Zeeman shift is the following:

$$\Delta E = -g_J \mu_B M_J B, \tag{2.10}$$

where g_J is the Lande g-factor derived from the precession of $\vec{L}$ and $\vec{S}$ around the total angular momentum, $\vec{J}$ [4]. Since we are considering the stretch states, states with maximum spin projection, we can directly evaluate the shift. We choose $\vec{B} = B \cdot \hat{z}$, such that $\vec{L} \cdot \hat{z} = L_z$ and $\vec{S} \cdot \hat{z} = S_z$ and therefore Equation (2.9) simplifies to

$$H' = \frac{\mu_B B}{\hbar}(L_z + 2S_z), \tag{2.11}$$

where μ_B is the Bohr magneton.

In order to find the Zeeman shift of the ground and excited states due to an external magnetic field, we write the ground and excited states of our slowing transition as:

$$|F = 3/2, M_F = 3/2\rangle = |L = 0, M_L = 0\rangle|S = 1/2, M_S = 1/2\rangle|I = 1, M_I = 1\rangle \tag{2.12}$$

$$|F = 5/2, M_F = 5/2\rangle = |L = 1, M_L = 1\rangle|S = 1/2, M_S, = 1/2\rangle|I = 1, M_I = 1\rangle \tag{2.13}$$

where $\vec{L}$ is the orbital angular momentum, $\vec{S}$ is the intrinsic spin of the electron, $\vec{I}$ is the nuclear spin and $\vec{F} = \vec{L} + \vec{S} + \vec{I}$ is the total angular momentum. To find the first-order perturbation, we evaluate the expectation value of our perturbation Hamiltonian on each state:

$$E_{excited} = \langle F = 5/2, M_F = 5/2|H'|F = 5/2, M_F = 5/2\rangle \tag{2.14}$$

$$E_{ground} = \langle F = 3/2, M_F = 3/2|H'|F = 3/2, M_F = 3/2\rangle \tag{2.15}$$

Substituting the perturbed component of our Hamiltonian, Equation (2.11), into

Equations (2.14) and (2.15) reveals

$$E_{excited} = \langle F = 5/2, M_F = 5/2 | \frac{\mu_B B}{\hbar}(L_z + 2S_z)|F = 5/2, M_F = 5/2\rangle \quad (2.16)$$

$$E_{ground} = \langle F = 3/2, M_F = 3/2 | \frac{\mu_B B}{\hbar}(L_z + 2S_z)|F = 3/2, M_F = 3/2\rangle \quad (2.17)$$

Calculating the expectation values yields:

$$E_{excited} = 2\mu_B B \quad (2.18)$$

$$E_{ground} = \mu_B B. \quad (2.19)$$

Finally, the shift in energy levels, $\Delta E = E_{excited}$ - E_{ground}, becomes

$$\Delta E = \mu_B B. \quad (2.20)$$

Equation (2.20) gives the relative energy shift of the ground and excited states as a function of magnetic field.

2.4 Magnetic Field Taper

Having calculated the shift in energy, we can calculate a magnetic field taper that will keep atoms on resonance with incoming photons. We first write the velocity of an atom as a function of position using the familiar kinematics equation

$$v^2(z) = v_i^2 + 2az, \quad (2.21)$$

where v_i is the initial velocity of the atoms and z is the position along the slower axis. To calculate the deceleration, we must first find the force on an atom from

incoming photon. The maximum scattering force is given by

$$F = -\frac{\hbar k \Gamma}{2m} \tag{2.22}$$

in the direction opposing the atom's forward trajectory, with $k = 2\pi/\lambda$ and $\Gamma/2$ equal to the spontaneous emission and absorption rate [8]. Applying Newton's second law,

$$a = -\frac{\hbar k \Gamma}{2m} \tag{2.23}$$
$$\approx -1.8 \times 10^6 m/s^2$$

In our experiment, this deceleration is 200,000 times as large as the acceleration due to gravity.

Next, we correlate our Zeeman energy shift with the Doppler shift by equating the respective frequencies:

$$\frac{\Delta E}{\hbar} = \frac{\mu_B B(z)}{\hbar} = kv(z). \tag{2.24}$$

We can now calculate a magnetic field taper that keeps atoms in constant resonance with incoming photons. We solve Equation (2.24) for B and substitute Equation (2.21) into the result:

$$B(z) = \frac{\hbar k}{\mu_B} \sqrt{v_i^2 - \frac{\hbar k \Gamma}{m} z}. \tag{2.25}$$

Figure 2.3 displays a graph of $B(z)$ with $v_i = 1100$ m/s. The quick drop in B-field at the end of the slower is necessary in order to quickly detune the atoms from resonance so that they do not drift backward into the slower.

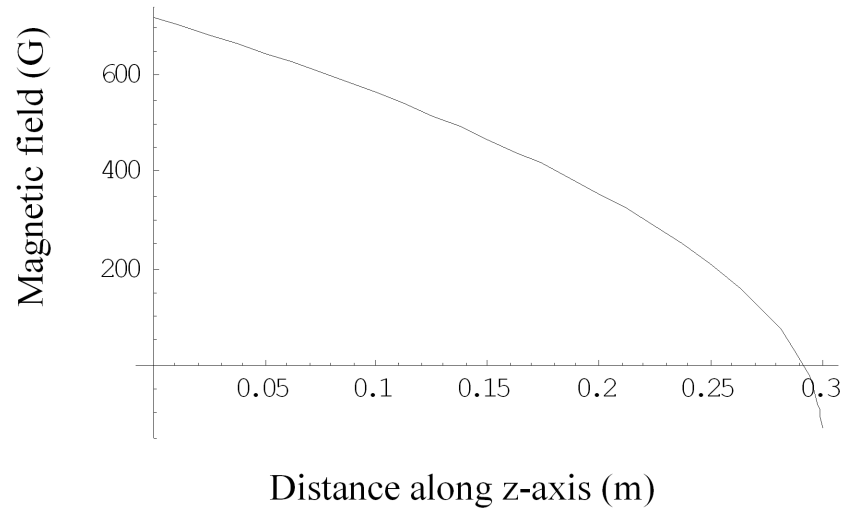Having thus derived a B-field taper, we are now able to design a Zeeman Slower

Figure 2.3: Desired magnetic field as a function of z.

to generate the magnetic field that will keep atoms in constant resonance with incoming photons.

2.5   Zeeman Slower

We use a Zeeman Slower to attain the desired magnetic field. The slower is composed of multiple electromagnets aligned along a common axis. When we run current through the electromagnets, we generate a magnetic field along the axis. The original Zeeman Slower, currently in use, is 60 cm long and is made up of 10 equally wound coil sections. In order to achieve the desired B-field taper, each coil is run at a unique current by ten independent power supplies. This design allows us to fine tune the magnetic field in each coil to optimize slowing. The original slower design necessitates water cooling and would be expensive to build and complicated to replicate for the new cooling and trapping system.

2.6 Design Modifications

In hopes of designing a more compact and cost efficient experimental apparatus, we modelled a shorter slower with tapered coils. Figure 2.4 illustrates the old and new design.
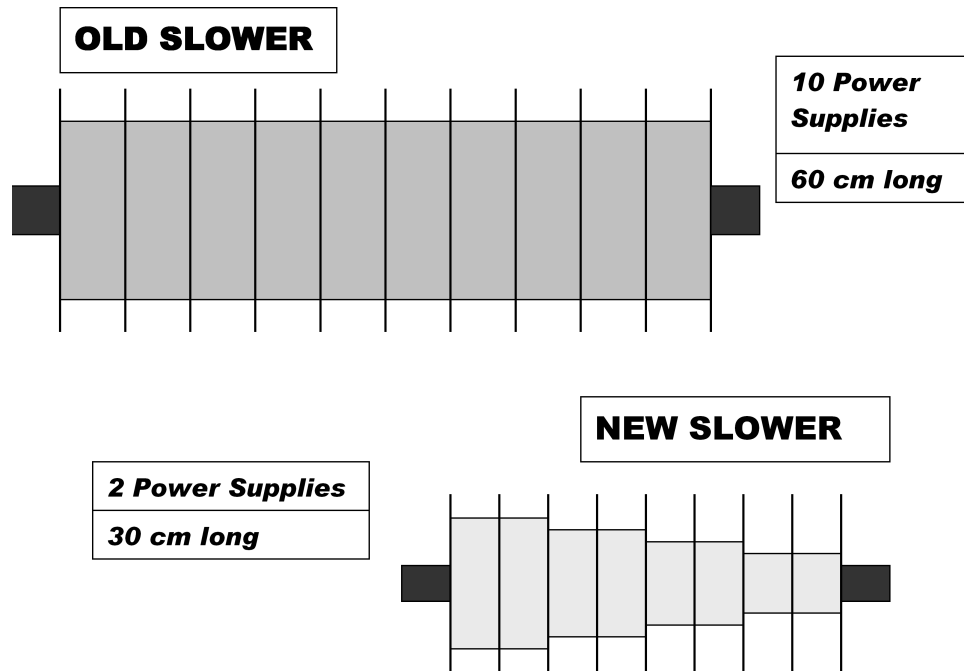

Figure 2.4: The old slower and the new design.

2.6.1 A Shorter Slower

In 2002, Margaret Harris explored building a shorter Zeeman Slower [9]. She concluded that a longer slower would produce more *slow* atoms but not more *trappable* atoms. Atoms have both a longitudinal velocity and a radial velocity as they leave the oven. As the atoms are laser cooled, their longitudinal velocity decreases, while their radial velocity remains unchanged. An atom's radial velocity will take it outside the MOT's capture radius if it travels for a long enough time.

Length (m)	Rate (atoms/s)
1	6.28×10^8
0.5	4.43×10^8
0.4	3.82×10^8
0.3	3.10×10^8
0.2	2.24×10^8
0.1	1.22×10^8

Table 2.1: Trap loading rates at selected values of slower length [9].

By using simple kinematics, we can compare the MOT loading rate with the length of our slower. As we can see from Table 2.1, long and short slowers have comparable loading rates. For loading times of one or two seconds, even a very short slower could saturate a ^{6}Li MOT which requires about 0.5×10^6 atoms [9].

In addition, Harris used Mathematica and our knowledge of a preferred B-field taper to calculate expected currents and an ideal length for a shorter slower. She compared the fit between the ideal and the experimental taper until she found the best fit for the shortest length. Harris concluded that a 30 cm slower with 8 coil segments could slow enough atoms, would cut the current requirements in half, and should not require water cooling [9].

2.7 Tapered Coils

Harris' work on a compact Zeeman Slower helped jump start our project. A 30 cm slower would be much easier to build and would take up less space on the lab table, but it still required 8 different power supplies. Building 8 new power supplies would take too much time while buying them would be too costly. Our hope was to build a slower which required two power supplies.

We chose to construct eight coil segments run by two power supplies instead of eight. To do this, we created the B-field taper with varied number of winds instead of varied currents for each coil segment. The first power supply would power the first seven coils connected in series, while the second would run a much smaller current in the opposite direction of the other seven coils to detune the ^{6}Li from resonance. Though this design would not be as flexible for fine tuning our B-field, we hoped through careful design and construction, we could build a functional slower. We chose to use two power supplies instead of one because the number of collected atoms is sens/itive to the amount of detuning in the last coil. The ability to fine tune the current in the last coil would allow us to maximize the number of slow atoms experimentally.

Chapter 3

A Virtual Slower

Before we built and tested the new slower, we used a working model of the coil distribution on Mathematica. This "virtual slower" allowed us to calculate how many winds per coil we needed to fit our theoretical B-field. It confirmed whether a single wind of wire, as compared to varying the current, provided sufficient resolution to give a smooth magnetic field, and it illustrated whether one power supply could deliver enough current to run the seven primary coils of the new slower.

3.1 Calculating Magnetic Field

A notebook created by Mike Ghem and Michael Stenner laid the foundation for our computer model, allowing us to calculate the magnetic field of a "coil." A coil is represented by its radius, longitudinal position, number of winds, and current (see Appendix A for details). Though the magnetic field calculation capacities of this notebook are powerful, the coil representation, which sets all of a coil's winds into a single volume, is not physically accurate. In reality, a physical "Coil" segment is composed of numerous winds each of which lies at a distinct radius and a distinct position on the longitudinal axis of the slower.

17

3.2 Ideal Coil Taper

To make our virtual coils more physically accurate, we divided the slower into eight segments. Each Coil represented one of the eight independent segments of wire. Borrowing from a notebook created by Margaret Harris, we encoded a segment with distinct winds at a relative radius and position on the z-axis, illustrated in Figure 3.1. We could now find the magnetic field of each Coil using Mathematica by adding up the magnetic field of each wind in the segment. By changing the number of winds, we could tweak the B-field distribution until we found a best fit with our ideal B-field as discussed in Chapter 2.

In order to find the number of winds needed to fit our desired B-field taper, we envisioned each Coil in cross section. The $\hat{z}$ is directed parallel, while $\hat{r}$ is directed perpendicular to the axis of the slower. Figure 3.2 depicts a Coil cross-section with "horizontal winds", the number of winds that fit in the $\hat{z}$ direction, and "vertical winds", the number of winds that fit in the $\hat{r}$ direction. We found that a slower 30 cm long, with 8 equal coil sections separated by copper discs, could fit 22 horizontal winds in each Coil section. To find the number of vertical rows that would give the closest fit to the desired magnetic field taper, we tweaked the distribution by changing the number of winds in each Coil segment.

As we can see from Figure 3.3, the constant winding model more accurately fits our desired B-field taper. However, our constant current model fits the taper surprisingly well and is close enough to slow the amount of atoms we need. Table 3.1 shows the results of our calculations, and Figure 3.4 displays the magnetic field strength and direction.
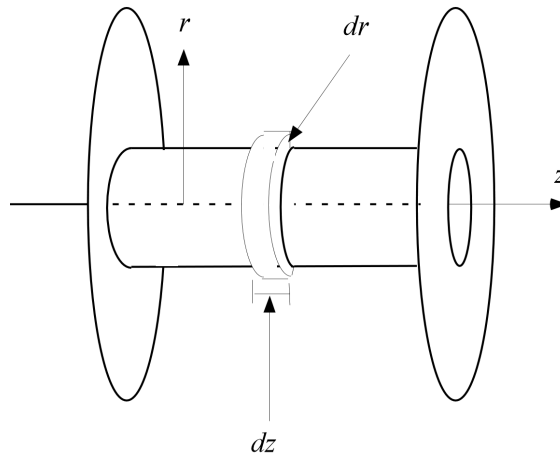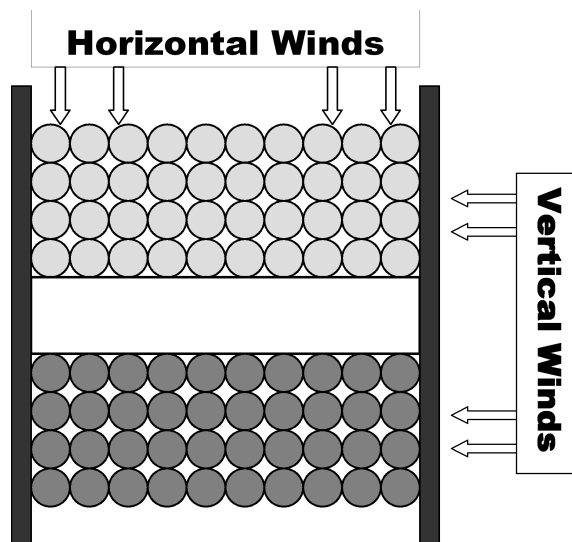
Figure 3.1: A virtual coil [9].

Figure 3.2: A cross-section of one Coil segment, depicting horizontal and vertical winds.

Coil Number	Vertical Windings	Horizontal Windings
Coil 1	13	22
Coil 2	10	22
Coil 3	9	22
Coil 4	8	22
Coil 5	7	22
Coil 6	5	22
Coil 7	4	22
Coil 8	4	22

Table 3.1: The number of horizontal and vertical winds and the dimensions of each wound Coil.

3.3   Voltage Requirements

Before we could consider our virtual model a success, we had to make sure our ideal slower did not require excessive voltage. We began by calculating the length of wire required for each Coil. Mathematica allowed us to sum up the circumference of each wind. Summing these values gave us a total length of 174 m (571 ft) for the first 7 coils. We did not include the last coil because it would be used to detune the atomic beam and would use a separate power supply.

Our best fit B-field was created using 9.5 Amps of current in the first 7 coils, and 14 AWG copper wire has a resistivity per foot of 0.002524 ohm/foot [10]. We found that the total resistance of the first 7 coils was 1.44 Ohms, using Ohm's Law, $V = IR$, This requires our power supply to output 13.7 Volts, a reasonable voltage for one power supply.
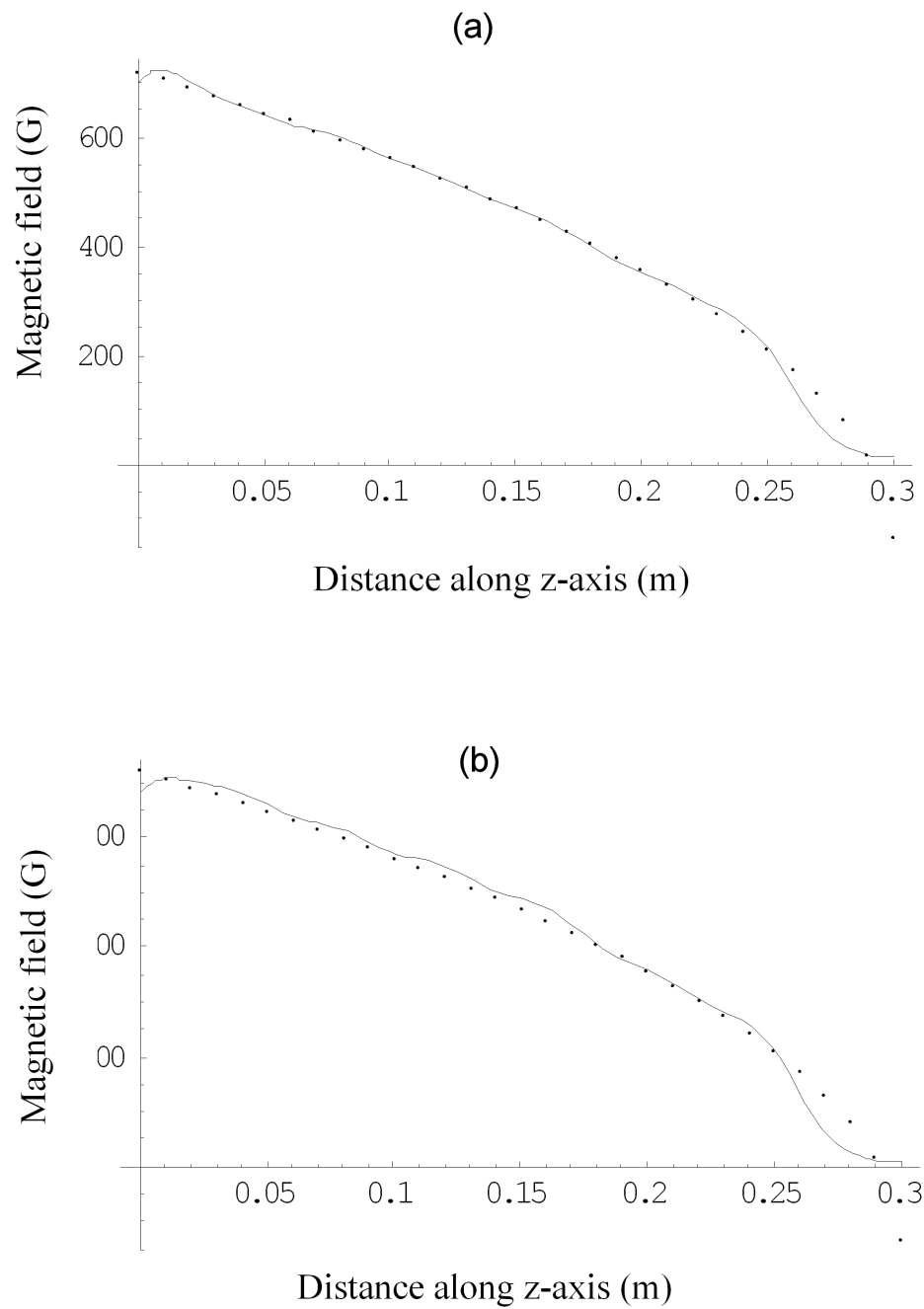
Figure 3.3: (a) A theoretical fit for a slower with constant winding and varying current [9]; (b) A theoretical fit for a slower with constant current and varied winding.
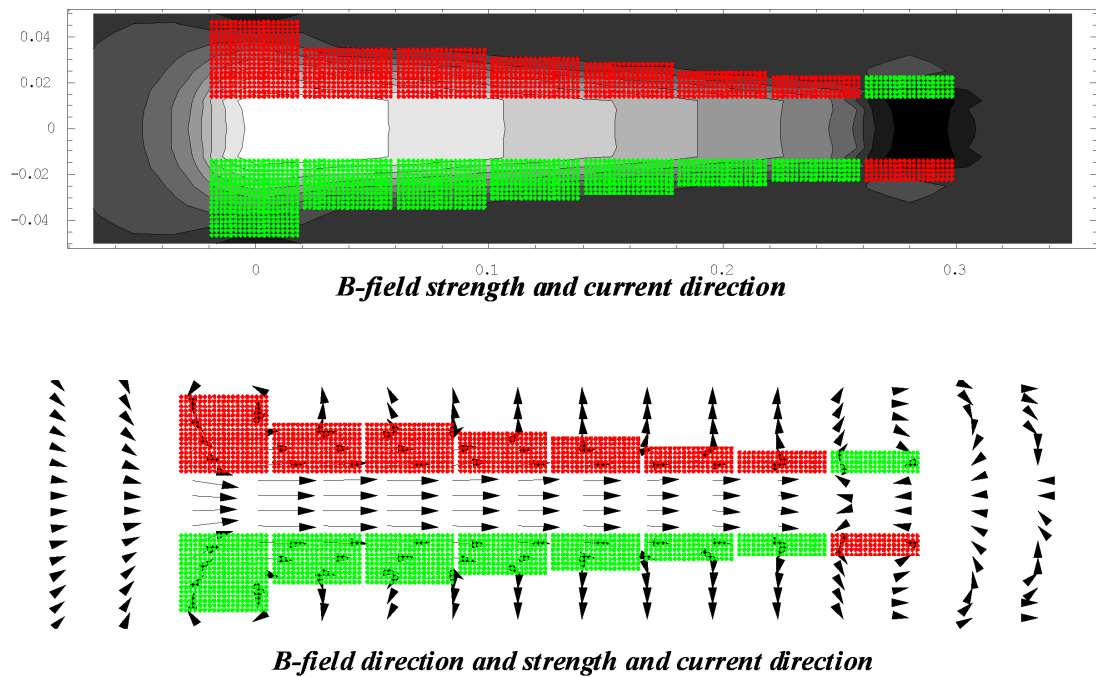
B-field strength and current direction

B-field direction and strength and current direction

Figure 3.4: A visual representation of our slower. In the first image, a white-to-black gradient represents decreasing magnetic field; in the second image, arrows denote the direction of the magnetic field.

Chapter 4

Construction

4.1 Main Body

We chose as the backbone for our slower a 30 cm long, 1 in O.D., #304 stainless steel pipe. To separate our eight main coil sections, we designed 5 in diameter discs. Cut from a 0.05 in copper sheet, they would be placed an equal distance apart along the length of our inner pipe. Stainless steel is a good material for an ultra high vacuum system, while the copper discs make a good heat sink.

We sent our TurboCad drawings of the slower design, included in Appendix 2, to the Duke Instrument Shop. The shop, headed by Robert Timberlake, devised a means to keep all nine discs perfectly spaced and perpendicular to the central axis. They cut eight aluminum blocks the width of the space between discs. After soldering on the first disc, they stacked on an aluminum block before soldering the next disc, keeping the discs perpendicular. They continued this process along the full length of the slower.

4.1.1 Conflat Flanges

To connect the slower to the experimental set-up, we attached a 2-3/4 Conflat Flange to each end of the stainless steel pipe. We chose one rotatable and one non-
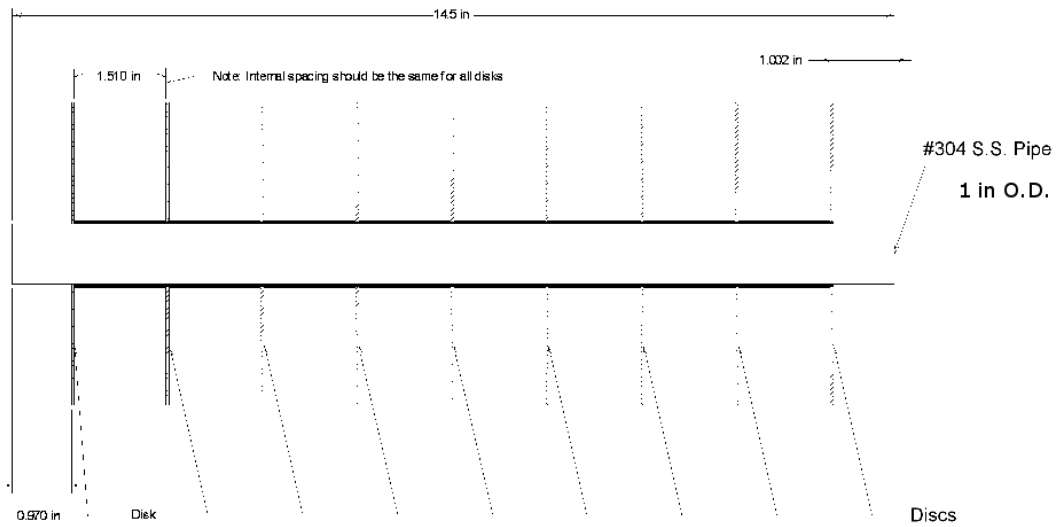
Figure 4.1: The layout of our slower design.

rotatable flange to ease the alignment process during installation. The stainless steel pipe was carefully cleaned with acetone and methanol before we asked Gary Swift, at Duke's Free Electron Laser Laboratory (FEL), to help out with the ultra high vacuum weld. After welding, we capped off both ends of the slower to keep the pipe free of contamination during the winding process.

4.2 Additional Parts

4.2.1 Brass Clamps

Concerned about the strength of the solder joints, we machined brass clamps that would fit around the central pipe on each side of a coil segment as it was wound. The force of the wound wire would be opposed by a clamp, releaving some of the pressure on each solder joint.
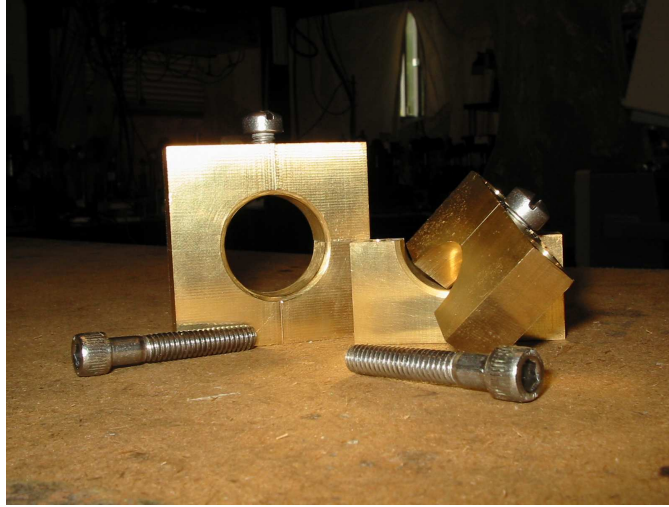
Figure 4.2: A photo of our brass clamps.

The clamp was constructed from a square brass block. We used a lathe to cut a circular hole in the center, matching the diameter of our stainless steel pipe. A small amount of brass was shaved off the circumference of each hole to allow the clamp to fit snugly over the welded joint. Holes were drilled to fit two screws which held the clamps together after they were cut in half. Figure 4.2 displays the finished clamps.

4.2.2   Retaining Bars

We made eight blocks to fill the space from the top of the winds to the top of the copper discs. The blocks were made of Delrin, an easily machinable plastic, and were designed in four distinct sizes to account for varying heights of wire (see Appendix 2). To each retaining Delrin bar, we added two allen bolts. The blocks had a two-fold purpose. They held down the wound wire which had a tendency to loosen, and they acted as ports to connect the Coils in series. Screws attached the blocks between two copper discs.

4.3 Winding

In order to wind the slower, we attached the slower skeleton to the lathe. This allowed us to wind the wire as we rotated the lathe by hand. Contrary to earlier work, which stated that the winding process becomes chaotic after a few layers, we found a way to keep the winds reasonably aligned with the help of a few custom-made tools and bit of patience. A more uniform winding job allowed us to more closely follow our theoretical calculations for the optimal number of winds per Coil segment.

We faced two difficulties. First, it was difficult to keep the wire flowing steadily as we rotated the slower from the large roll. Second, it was difficult to align the wire so it flowed on perfectly perpendicular to fit the desired number of winds per layer. We noticed that in order to follow our theoretical winding, we would have to force each wind in place between the copper discs.

4.3.1 Tools

We designed a chisel like tool, made of Delrin. This tool allowed us to force into place each wind. The Delrin kept us from scratching off the insulating coating of our wire. We also created a guiding tool, a small Delrin block through which we drilled a hole slightly bigger than the diameter of the wire. Feeding wire through the tool, we could apply downward pressure allowing the wire to slide onto a Coil more smoothly. The block helped us guide the wire and keep it untangled.
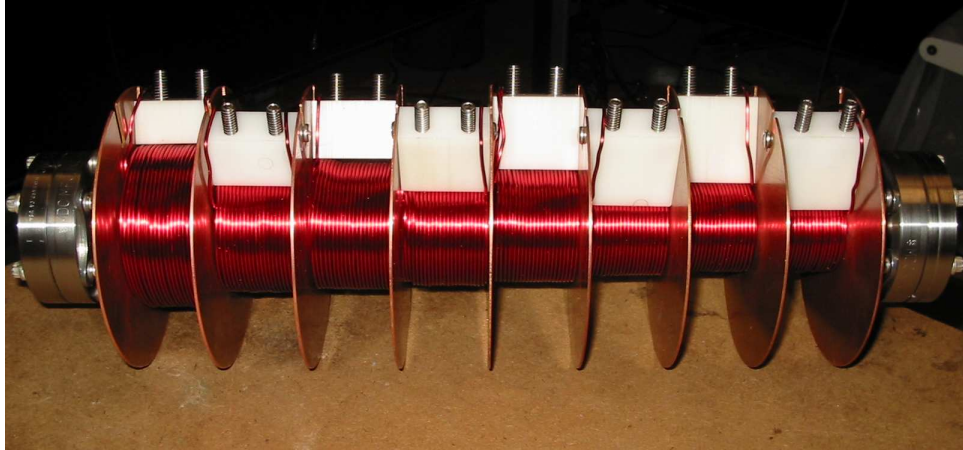
Figure 4.3: A photo of our wound Zeeman Slower.

4.3.2 Process

With the slower attached to a lathe, our initial impulse was to pulse the lathe and allow this action to pull the wire onto each Coil. Unfortunately, even a short pulse pulled too much wire, quickly making the winding process chaotic. In order to carefully align each wind, we rotated the lathe by hand.

To account for experimental error, we left about 10 ft of extra wire on each coil. It would be easy to cut this off at the end but impossible to add wire if a segment proved to have too little wire. Though tedious and time consuming, this process allowed us to create uniformly wound Coils, compatible with our theoretical description.

4.3.3 Results

Having finished the winding process, we found that coils four and five were shorting out. After investigating, we found silver solder residue on the central pipe was scratching off the coating of our wire. Sanding down the excess solder and rewinding the affected coils fixed the problem. Figure 4.3 displays our finished Zeeman Slower.
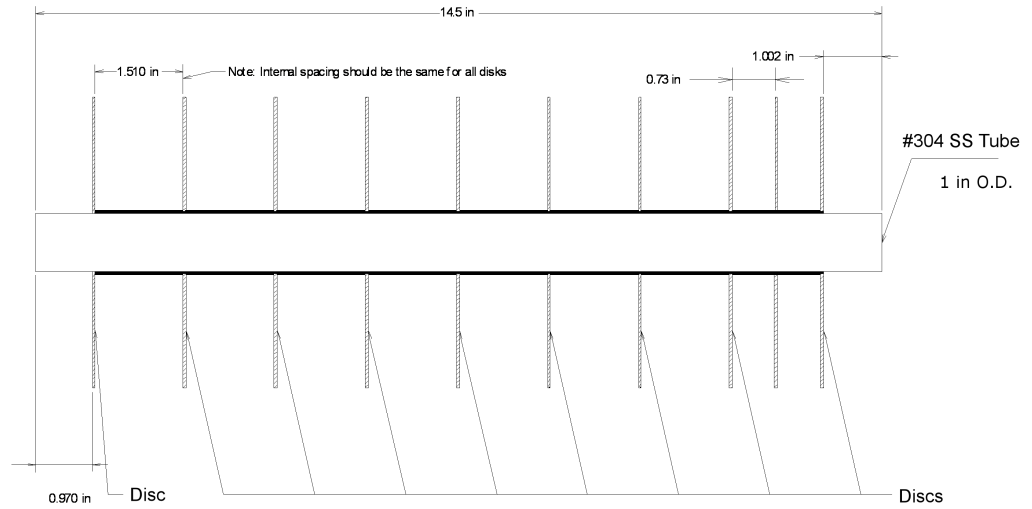
Figure 4.4: The layout with an additional copper disc.

4.4 Modifications

We designed the slower to have seven Coils running on one primary power supply and the eighth Coil running backwards on a separate supply. This was necessary to keep the atoms from being pushed back into the slower, as they continued to be slowed by the laser beam.

The detuning proved to be too abrupt, so we separated the eighth coil into two independent coils separated by an extra copper disc. The first half of the eighth Coil was to be connected in series with the first seven while the second half of the Coil was to become the detuning coil. Figure 4.4 details the addition of an extra copper disc. This modification should be taken into account in any future duplication of this design.

Chapter 5

Testing

5.1 Preliminary Testing

Initial testing of the slower took place in two stages. First, we tested the temperature distribution to be assured the slower would not need water cooling. Second, we tested the magnetic field using a magnetic field probe to compare the actual magnetic field taper with our theoretical plot.

5.1.1 Temperature Distribution

We designed our slower in hopes that it would not need water cooling, and we needed to confirm our calculations before moving on. Our first test at 10 Amps produced a slower hot to the touch. Worried about the condition of our wire coating, we set up two fans on the four largest Coils to help keep down the temperatures.

To test the temperature distribution, thermocouples were set up on the first, second and seventh Coils. We later found that the thermocouples had scratched the wire of one of our Coils causing it to short out and forcing us to rewind. Protecting the slower from such scratches should be a high priority for all future construction and design. We began with 5 Amps to be safe and increased this to 10 Amps once we saw that temperatures remained in a harmless range for our wire. We wished

to avoid temperatures over 90°C, but after a few hours the coils remained around
50°C temperatures, Typical temperature fluctuations were only a few degrees. Our
compact slower did not require water cooling.

5.1.2   Magnetic Field

In order to test and optimize the magnetic field, we secured the slower at a level
height off of the lab table with two clamp-like mounts. The rotatable Conflat flange,
allowed the apparatus to rotate on its long axis, permitting us to easily unwind Coils
if we needed to adjust the field. We mounted a Gauss meter at a height compatible
with the center axis of the slowing tube and secured an aluminum strip on the lab
table. The Gauss meter could move along this strip without varying its horizontal
position within the slower. A meter stick taped to the lab table allowed us to keep
track of the distance along the long axis.

We first measured the magnetic field of each of the eight Coils separately. Our
"Virtual Slower" calculations in Mathematica allowed us to calculate the desired B-
field in each segment. Running 1 Amp through each Coil, we unwound the necessary
number of winds to achieve our theoretical magnetic field per amp. To achieve the
correct B-field, our largest Coil required a total of 297 turns - our theory had
predicted 299. Surprisingly, after the fine tuning process, each Coil was within two
or three turns of the theory. This proved that the slower could be very consistently
wound.

Next we measured the magnetic field distribution of the entire slower. The power
supply was set up in series along the length of the slower, including the first seven
Coils and the first half of the eighth Coil. Beginning a few inches before the first
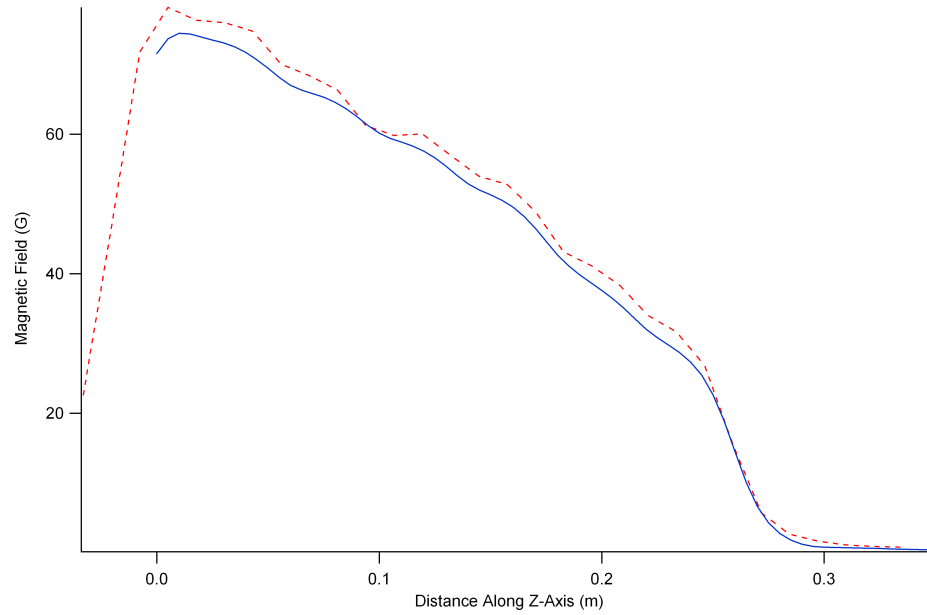Coil, we started taking B-field measurements every 0.25 inches. Figure 5.1 displays

Figure 5.1: A graph comparing our experimental (dotted line) and theoretical (solid line) B-field data.

our experimental data (dotted line) vs. the theoretical data (solid line). The results surpassed our expectations, and we were ready to test whether our compact air-cooled slower could slow atoms. The slower was run at 10 Amps, requiring 17 Volts, proving that our voltage predictions were accurate.

5.2   MOT Loading

Our final challenge was to test if our slower could produce enough trappable atoms. We set-up and optimized a new oven and vacuum system. We then laid out the optics for our system. For our experiment, we used a Coherent model 699-21 ring dye laser and a Coherent model 899-21 ring dye laser. The 699 provided our slowing beam which opposed the motion of the atomic beam. The 899 provided our probe beam, which intersected the atomic beam at a 45 degree angle, once the atoms
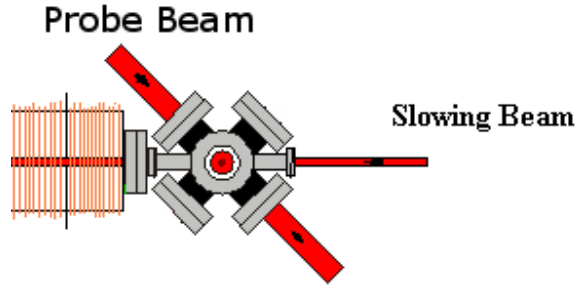
Figure 5.2: The intersection of beams at the eight-way cross.

traversed the length of the slower. A PMT - photomultiplier tube - was installed at the top window of our eight-way cross chamber to detect fluorescence. Figure 5.2 displays the layout of our beams.

In the slowing beam, we set up a "repumper" to excite the atoms that decay to the $2S_{1/2}(F = 1/2)$ ground state from the $2P_{3/2}(F = 3/2)$ excited state. We also added a quarter waveplate to circularly polarize the beam, singling out our desired $2S_{1/2}(F = 3/2, M_F = 3/2) \rightarrow 2P_{3/2}(F' = 5/2, M_{F'} = 5/2)$ transition. In the probe beam, we added a beam chopper to lock-in detect the signal fluorescence from the slowing beam. For a full description of the experimental set-up, see [6] and [8].

A Mathematica program written by Le Luo allowed us to quantify the velocity distribution from our fluorescence data received by the PMT. Figure 5.3 shows the final velocity of ^{6}Li after the atoms have traveled the full length of the slower. We can see that a large number of atoms are cut from a velocity 1000 m/s to about 100 m/s.

Our final step was to set up the necessary optics to create a MOT. After weeks of fine tuning, we successfully proved that our compact air-cooled slower could successfully slow enough atoms to capture in a MOT.
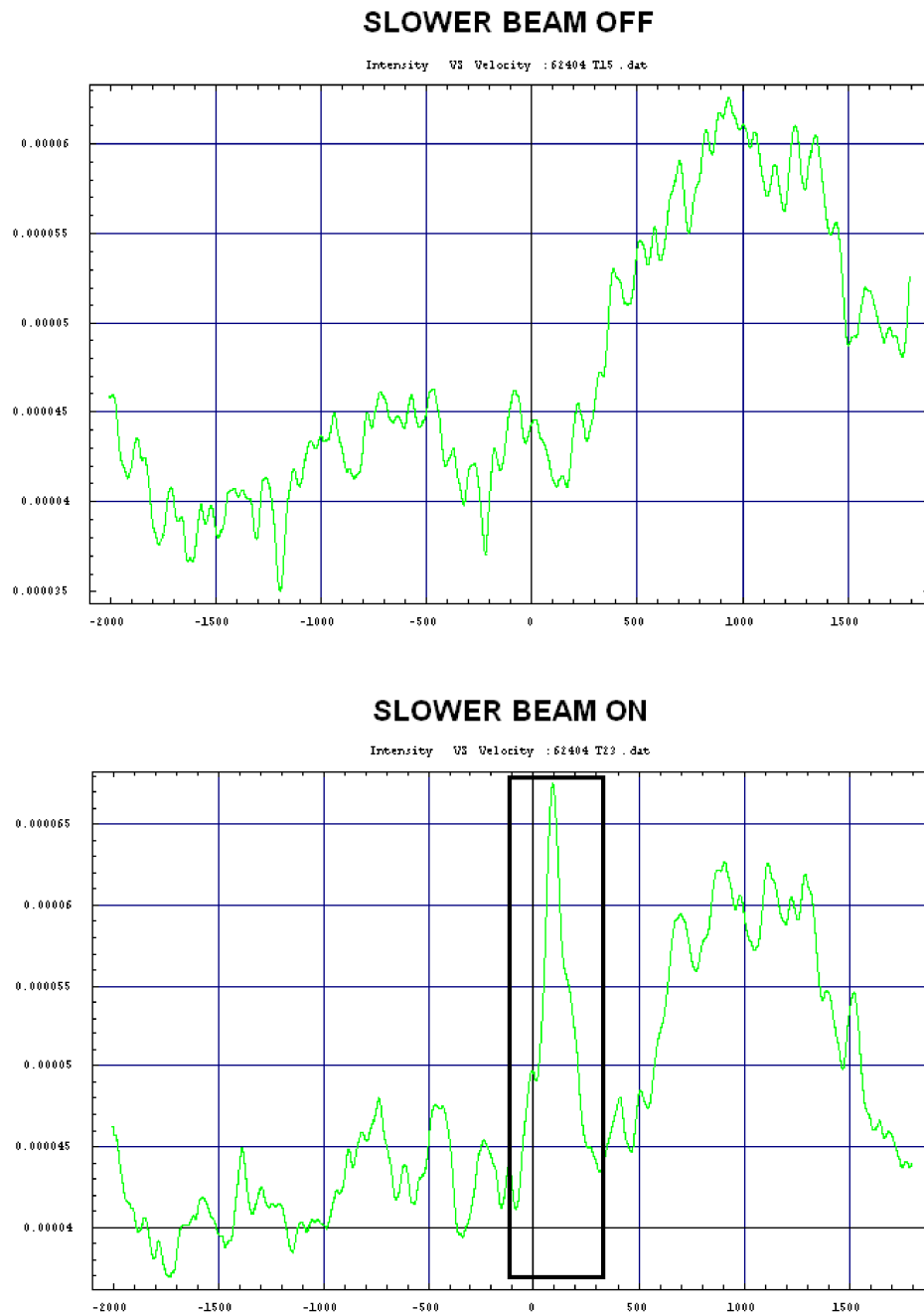
SLOWER BEAM OFF

Intensity VS Velocity : 52404 T15 .dat

SLOWER BEAM ON

Intensity VS Velocity : 52404 T23 .dat

Figure 5.3: The ^{6}Li velocity distribution with the slower on and off. The boxed element represents slowed atoms.

Chapter 6

Conclusion

The goal of this project was to design, construct, and test a compact and air-cooled Zeeman Slower. The new design would run on two power supplies instead of ten, would not require water cooling, and would be simpler to construct and operate than the current design. The construction of the new slower was to be the first step in a larger project aimed at designing a new and improved experimental set-up in our lab.

Testing of the new compact slower confirmed our theoretical predictions. The magnetic field taper created by tapered coils and constant current was consistent with the field produced by our old design. In addition, the slower did not require water cooling and could successfully slow atoms to trapping velocities.

A new and improved experimental set-up, which includes our new Zeeman Slower, has been running experiments since 2005. Our compact slower appears to be a reliable source of cold atoms. We are currently in the process of constructing a second Zeeman Slower, which mimics the design discussed in this document. Our hope is to replace the original Zeeman Slower in our older laboratory with an updated model in the near future.

Appendix A

Mathematica Code

I. Length

Setting up length equations:
```
vzmax[l_] := Sqrt[vf^2 + 2*a*l]
vrmax[l_] :=
  r0 / ((vzmax[l] - vf) / a + df / vf + di / vzmax[l])
vrmax[.3]
0.634352
r[l_] := 4*10^15* (1 - Exp[(-vzmax[l]^2) / alpha^2])
    (1 - Exp[(-vrmax[l]^2) / alpha^2])
```
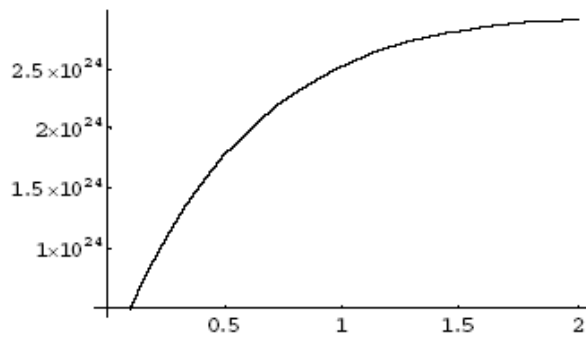
Setting parameters:
```
alpha = 1363
1363
r0 = .01
0.01
vf = 10
10
a = .75 * 1.83*10^6
1.3725×10^6
df = .15
0.15

di = .10
    0.1
```

Graphing r[l], the trap loading rate:
```
Plot[4*10^15*r[l], {l, .1, 2}]
```

. Graphics .

Calculating R for sample lengths l:

r[.1]
1.22112×10^8
r[.2]
2.24452×10^8
r[.5]
4.43091×10^8
r[.05]
6.36009×10^7
r[.3]
3.10268×10^8
r[.4]
3.82403×10^8

II. Magnetic Field Modeling

Code in existing Mathematica notebook:

Definitions
Constants
$\mu 0 = 4\,Pi * 10\,\hat{}\,{-3};$ (* Gives answers in Gauss *)
Calculation Functions
These functions calculate the radial and axial field for a single coil.

```
Bz[r_, z_, coil_] :=
 coil[[3]] * coil[[4]] * (μ0 / (2 Pi)) / √((coil[[1]] + r)² + (z - coil[[2]])²) *
 (EllipticK[ (4 coil[[1]] r) / ((coil[[1]] + r)² + (z - coil[[2]])²) ] +
  ( (coil[[1]]² - r² - (z - coil[[2]])²) / ((coil[[1]] - r)² + (z - coil[[2]])²) ) *
  EllipticE[ (4 coil[[1]] r) / ((coil[[1]] + r)² + (z - coil[[2]])²) ])
Br[r_, z_, coil_] := coil[[3]] * coil[[4]] * z^2 *
 (μ0 / (2 Pi r)) / √((coil[[1]] + r)² + (z - coil[[2]])²) *
 (-EllipticK[ (4 coil[[1]] r) / ((coil[[1]] + r)² + (z - coil[[2]])²) ] +
  ( (coil[[1]]² + r² + (z - coil[[2]])²) / ((coil[[1]] - r)² + (z - coil[[2]])²) ) *
  EllipticE[ (4 coil[[1]] r) / ((coil[[1]] + r)² + (z - coil[[2]])²) ])
```

These functions calculate the field for all of the coils listed in "coils".

```
AxialField[r_, z_, coils_] :=
 Module[{}, TempFunc[coil_] := Bz[r, z, coil];
  Plus @@ Map[TempFunc, coils, {1}]]
RadialField[r_, z_, coils_] :=
 Module[{}, TempFunc[coil_] := Br[r, z, coil];
  Plus @@ Map[TempFunc, coils, {1}]]
```

This function calculates the field magnitude at any point using the previous functions.

```
FieldMag[r_, z_, coils_] :=
 If[r == 0, AxialField[r, z, coils],
  √(AxialField[r, z, coils]² + RadialField[r, z, coils]²)]
```

Tools for generating "coils" list

```
WithTurns[precoil_, turns_] :=
 Module[{}, TempFunc[coil_] := Append[coil, turns];
  Map[TempFunc, precoil, {1}]]
WithCurrent[precoil_, current_] :=
 Module[{}, TempFunc[coil_] := Append[coil, current];
  Map[TempFunc, precoil, {1}]]
WithTurnsAndCurrent[precoil_, turns_, current_] :=
 WithCurrent[WithTurns[precoil, turns], current]
```

Description

What this notebook does
This notebook calculates the magnetic field at any point in space for an arbitrary number of coils. Each coil can have a different position, size, number of turns, and current. The one restriction is that all coils must share the same axis.

How to use this notebook
First, you must make your "coils" list. This is a list of lists. You have one internal list for each coil. Each of these internal coil (singular) lists contains the radius of the coil (in meters), the position of the coil (in meters), the number of turns, and the current (in Amperes). The following coils list defines one coil with a radius of 10 cm, position of z = 5 cm, 100 turns, and a 1 mA current.

```
ExampleCoils = {{.1, .05, 100, .001}};
```

Once this is defined, you can determine the axial field (parallel to z), radial field (perpendicular to z), and field magnitude at any point (r, z) with the functions: AxialField, RadialField, and FieldMag. each of these functions takes r, z, and your coils list. All of these functions return the magnetic field in Gauss. Example:

```
Plot[AxialField[0, z, ExampleCoils], {z, -.1, .1}];
```
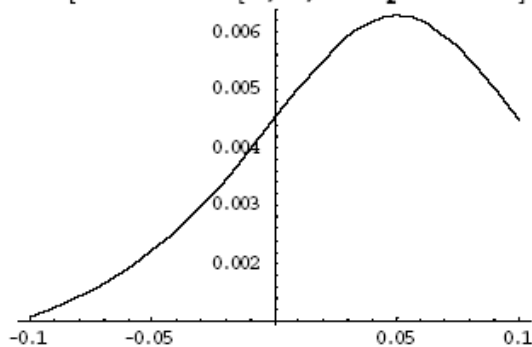

Generating coils lists
There are several functions to help you generate coils lists.

The function "Helmholtz" takes the parameters for a coil list (r, z, turns, current) and returns a coils list with two identical coils. One has the parameters you specified, and the other has a position of -z.

The function "TrueHelmholtz" takes the same parameters except that it does not take a radius. The radius is automatically set to 2z.

The functions "AntiHelmholtz" and "TrueAntiHelmholtz" work identically except that the mirror coil has the opposite current.

```
ExampleCoils = AntiHelmholtz[.4, .15, 100, .001];
Plot[AxialField[0, z, ExampleCoils], {z, -.1, .1}];
```
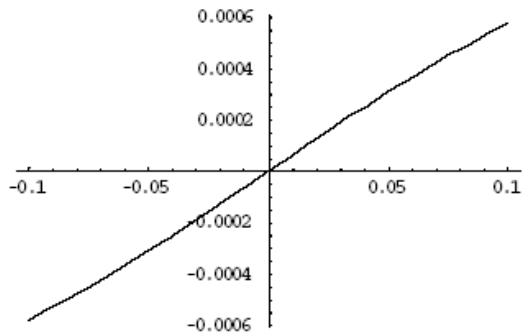
There are also functions for helping generate a list of several coils with the same current or number of turns. To use these functions, create a "precoils" list without the current or without both current and turns.

```
ExamplePreCoils = {{.1, -.1}, {.1, .1}}
{{0.1, -0.1}, {0.1, 0.1}}
NewExamplePreCoils = WithTurns [ExamplePreCoils , 30]
{{0.1, -0.1, 30}, {0.1, 0.1, 30}}
ExampleCoils = WithCurrent [NewExamplePreCoils , .4]
{{0.1, -0.1, 30, 0.4}, {0.1, 0.1, 30, 0.4}}
```
Or simply
```
ExampleCoils = WithTurnsAndCurrent [ExamplePreCoils , 30, .4]
{{0.1, -0.1, 30, 0.4}, {0.1, 0.1, 30, 0.4}}
```

Function Summary

coils =
coils = Helmholtz[rad, z, turns, I]
coils = TrueHelmholtz[z, turns, I]
coils = AntiHelmholtz[rad, z, turns, I]
coils = TrueAntiHelmholtz[z, turns, I]
coils = WithCurrent[precoils, I]   (where precoils is a coils list with the current missing)
precoils = WithTurns[preprecoils, turns]   (where preprecoils is a coils list with both currents and turns missing)

AxialField[r, z, coils]
RadialField[r, z, coils]
FieldMag[r, z, coils]

Example

List of coils. Each coil is a list of (coil radius, coil z position, number of turns, and current). Distances are in meters, and current in Amperes.

```
coils = Helmholtz [12.25 * .0254 , 6.125 * .0254 , 30, 1];
RadiusOfInterest   = .1;
Plot [AxialField [0, z, coils ],
  {z, -RadiusOfInterest  , RadiusOfInterest }, PlotRange → All];
Plot [AxialField [r, 0, coils ], {r, -RadiusOfInterest  , RadiusOfInterest },
  PlotRange → All];
```
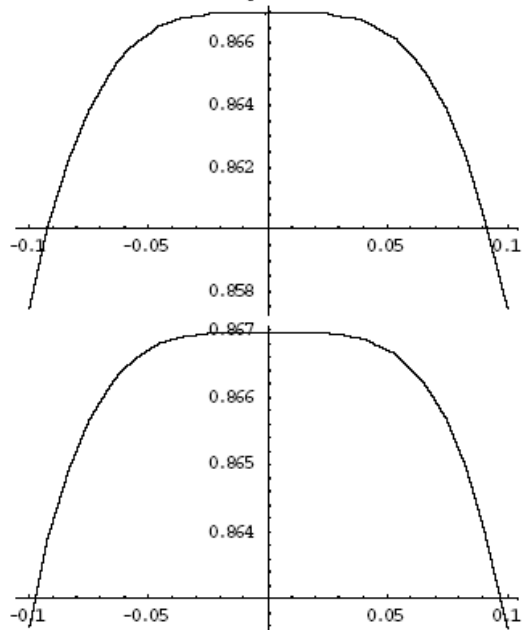

Modifications to Existing Notebook:

Setting up the iterated coils:
```
RegularSpacedRealCoil[InitR_, RStep_, RNum_, InitZ_, ZStep_, ZNum_, Current_] :=
  Flatten[Table[{InitR+ i* RStep, InitZ+ j* ZStep, 1, Current}, {i, 0, RNum - 1},
    {j, 0, ZNum - 1}], 1]
```

Defining constants and expressions for velocity and B-field:

```
h = 6.626 * 10^-34;
delta = -200 * 10^6;
lambda = 671.0 * 10^-9;
MB = 9.27 * 10^-28;
a = .6 * 1.83 * 10^6;
vf = 10;
l = .3

InitV[vf_, l_, a_] := Sqrt[vf^2 - l * 2 * -a];
bz[z_] := (h / MB) * (delta + (1 / lambda) * Sqrt[InitV[vf, l, a]^2 - (2 * a * z)])
Plot[bz[z], {z, 0, .3}]
data = Table[{z, bz[z]}, {z, 0, .3, .01}];
```

Use Nonlinear Fit package
Building the virtual slower, coil by coil:

```
<< Statistics`NonlinearFit`
SRad = 0.0125;
RInc = .002032;
RTurn = 17.0;
SZInc = .002032;
SZTurn = 19.0;
SingleCoil1 = RegularSpacedRealCoil[SRad, RInc, RTurn, -.019, SZInc, SZTurn, 1];
SingleCoil2 = RegularSpacedRealCoil[SRad, RInc, RTurn, .0211, SZInc, SZTurn, 1];
SingleCoil3 = RegularSpacedRealCoil[SRad, RInc, RTurn, .0612, SZInc, SZTurn, 1];
SingleCoil4 = RegularSpacedRealCoil[SRad, RInc, RTurn, .1013, SZInc, SZTurn, 1];
SingleCoil5 = RegularSpacedRealCoil[SRad, RInc, RTurn, .1414, SZInc, SZTurn, 1];
SingleCoil6 = RegularSpacedRealCoil[SRad, RInc, RTurn, .1815, SZInc, SZTurn, 1];
SingleCoil7 = RegularSpacedRealCoil[SRad, RInc, RTurn, .2216, SZInc, SZTurn, 1];
SingleCoil8 = RegularSpacedRealCoil[SRad, RInc, RTurn, .2617, SZInc, SZTurn, 1];
```

Test plot: what does a single coil's magnetic field look like?

```
Plot[AxialField[0, z, SingleCoil1], {z, 0, .1}]
```
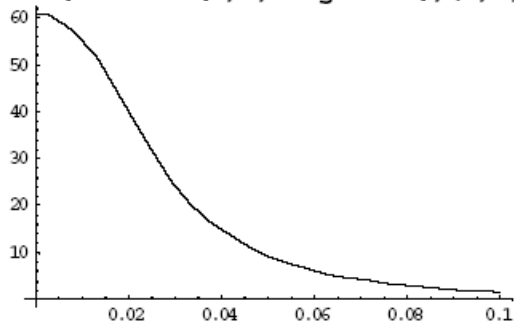

- Graphics -

Defining magnetic fields for each coil using the AxialField function:

```
B1[z_] := AxialField[0, z, SingleCoil1]
B2[z_] := AxialField[0, z, SingleCoil2]
B3[z_] := AxialField[0, z, SingleCoil3]
B4[z_] := AxialField[0, z, SingleCoil4]
B5[z_] := AxialField[0, z, SingleCoil5]
B6[z_] := AxialField[0, z, SingleCoil6]
B7[z_] := AxialField[0, z, SingleCoil7]
B8[z_] := AxialField[0, z, SingleCoil8]
Bfield[i1_, i2_, i3_, i4_, i5_, i6_, i7_, i8_] :=
  i1*B1[z] + i2*B2[z] + i3*B3[z] + i4*B4[z] + i5*B5[z] + i6*B6[z] +
   i7*B7[z] + i8*B8[z]
Clear[i1, i2, i3, i4, i5, i6, i7, i8]
```

Performing the nonlinear regression, output of values:
```
NonlinearRegress[data, Bfield[i1, i2, i3, i4, i5, i6, i7, i8], {z},
 {i1, i2, i3, i4, i5, i6, i7, i8}]
BestFitParameters → {i1 → 9.34725, i2 → 6.60703, i3 → 6.15811,
   i4 → 5.28855, i5 → 4.61755, i6 → 3.44819, i7 → 3.12214, i8 → -0.475744},
```

Using the best-fit currents to plot the simulated magnetic field:

```
p1 = Plot[9.35*B1[z] + 6.61*B2[z] + 6.16*B3[z] + 5.29*B4[z] + 4.62*B5[z] +
    3.44*B6[z] + 3.12*B7[z] + -.48*B8[z], {z, 0, .3}]
```



```
- Graphics -
```
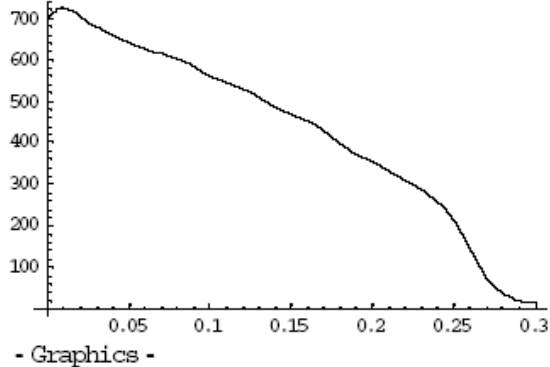
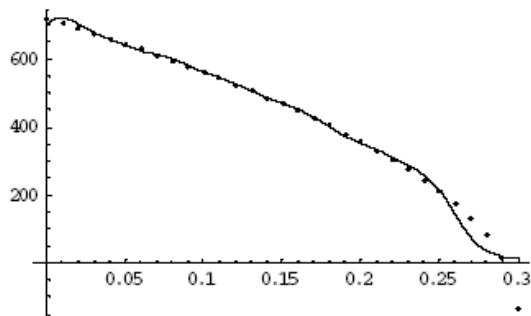Plot of the desired magnetic field taper:

```
p2 = ListPlot[data]
```
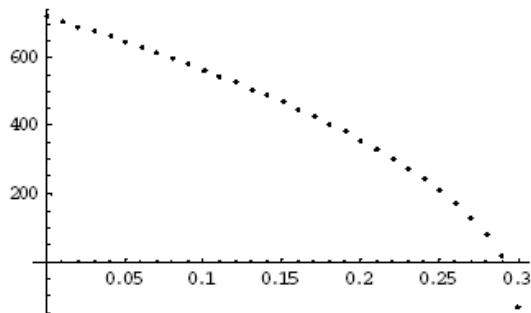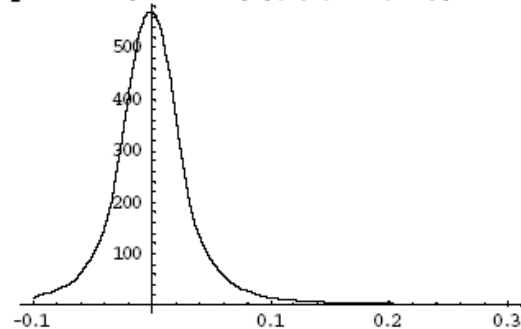
- Graphics -

Simulated (best-fit) magnetic field and ideal magnetic field:

Show[p1, p2]

Plot of the maximum-current coil at 9.35 A (part of prototype-testing process):

p3 = Plot[9.35 * B1[z], {z, -.1, .3}]

- Graphics -

Calculating the maximum magnetic field of this coil at 9.35 A:
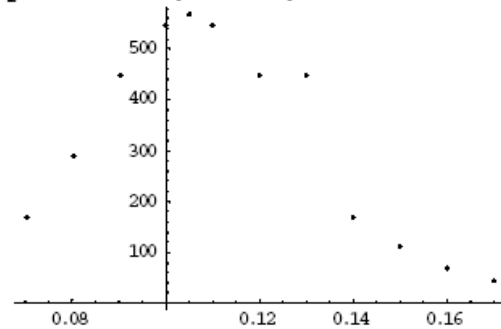
9.35 * B1[-0.001]
570.782

Comparing the prototype data with the simulation:

```
realdata = {{.17, 45}, {.16, 68}, {.15, 110}, {.14, 170}, {.13, 450},
   {.12, 450}, {.11, 550}, {.105, 570}, {.1, 550}, {.09, 450}, {.08, 290},
   {.07, 170}}
{{0.17, 45}, {0.16, 68}, {0.15, 110}, {0.14, 170}, {0.13, 450}, {0.12, 450},
 {0.11, 550}, {0.105, 570}, {0.1, 550}, {0.09, 450}, {0.08, 290}, {0.07, 170}}
```
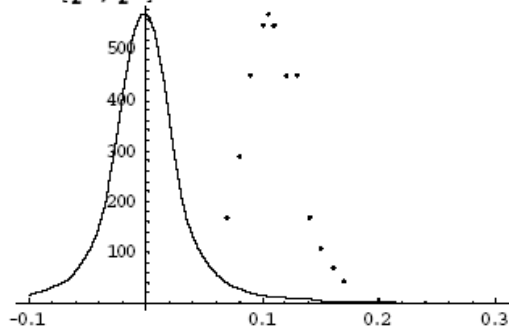
```
p4 = ListPlot[realdata]
```


- Graphics -

Prototype data and simulation on same graph:

```
Show[p3, p4]
```


- Graphics -

Further Modifications to Existing Notebook:

Setting up a template for a coil with a specified number of vertical winds:

```
RealCoil[R_,DeltaR_,NumR_,Z_,DeltaZ_,NumZ_,Amps_]:=Flatten[T
able[{R+i*DeltaR,Z+j*DeltaZ,1,Amps},{i,0,NumR-1},{j,0,NumZ-
1}],1]
```

Defining constants and number of vertical and horizontal winds per coil:

```
SRad=.015113;
RInc=.001679;
RTurn1=13;
RTurn2=10;
RTurn3=9;
RTurn4=8;
RTurn5=7;
RTurn6=5;
RTurn7=4;
RTurn8=4;
SZInc=.001679;
SZTurn=23.0;
```

Creating each separate coil unit:

```
Coil1=RealCoil[SRad,RInc,RTurn1,-.019,SZInc,SZTurn,1];
Coil2=RealCoil[SRad,RInc,RTurn2,.0211,SZInc,SZTurn,1];
Coil3=RealCoil[SRad,RInc,RTurn3,.0612,SZInc,SZTurn,1];
Coil4=RealCoil[SRad,RInc,RTurn4,.1013,SZInc,SZTurn,1];
Coil5=RealCoil[SRad,RInc,RTurn5,.1414,SZInc,SZTurn,1];
Coil6=RealCoil[SRad,RInc,RTurn6,.1815,SZInc,SZTurn,1];
Coil7=RealCoil[SRad,RInc,RTurn7,.2216,SZInc,SZTurn,1];
Coil8=RealCoil[SRad,RInc,RTurn8,.2617,SZInc,SZTurn,1];
```

Calculating the magnetic field for each coil:

```
B1[z_]:=AxialField[0,z,Coil1]
B2[z_]:=AxialField[0,z,Coil2]
B3[z_]:=AxialField[0,z,Coil3]
B4[z_]:=AxialField[0,z,Coil4]
B5[z_]:=AxialField[0,z,Coil5]
B6[z_]:=AxialField[0,z,Coil6]
B7[z_]:=AxialField[0,z,Coil7]
B8[z_]:=AxialField[0,z,Coil8]
```

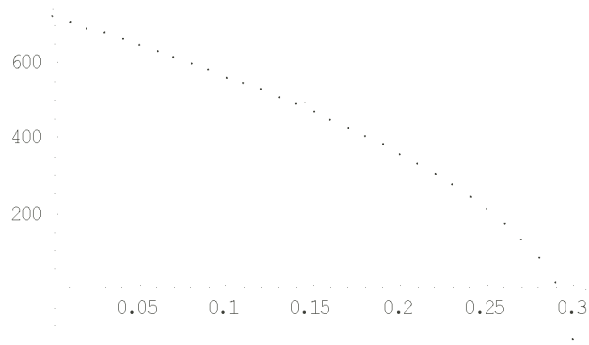Creating a total B-field taper and plotting versus the desired B-field:

```
Bfield[i1_,i2_,i3_,i4_,i5_,i6_,i7_,i8_]:=i1*B1[z]+i2*B2[z]+i
3*B3[z]+i4*B4[z]+i5*B5[z]+i6*B6[z]+i7*B7[z]+i8*B8[z]
 Clear[i1,i2,i3,i4,i5,i6,i7,i8]

NonlinearRegress[data,Bfield[i1,i2,i3,i4,i5,i6,i7,i8],{z},{i
1,i2,i3,i4,i5,i6,i7,i8}];

plot1=Plot[9.5*B1[z]+9.5*B2[z]+9.5*B3[z]+9.5*B4[z]+9.5*B5[z]
+9.5*B6[z]+9.5*B7[z]+-.55*B8[z],{z,0,.3}];
```
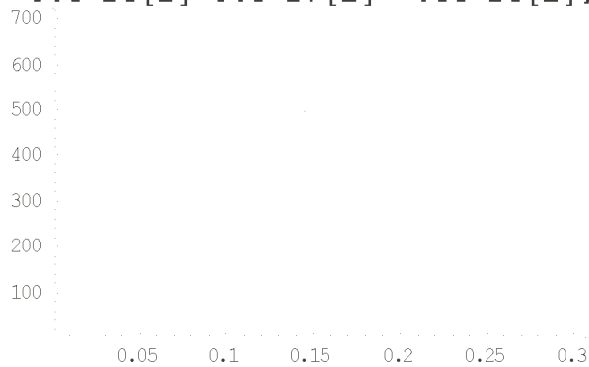


```
 Show[plot1,plot2];
```


Calculating total length of wire needed for slower:
```
(RTurn1/17)*9.5
 7.26471
 (RTurn2/17)*9.5
 5.58824
 (RTurn4/17)*9.5
 4.47059
 (RTurn5/17)*9.5
 3.91176
 (RTurn6/17)*9.5
 2.79412
 (RTurn7/17)*9.5
 2.23529
```

```
LengthOfOneWire[coil_]:=Apply[Plus,Take[Flatten[coil],{1,(Le
ngth[coil]*4),4}]*2 Pi]
 LengthOfOneWire[Coil1]
```
47.3181

```
LengthOfAllWires[coil1_,coil2_,coil3_,coil4_,coil5_,coil6_,c
oil7_]:=LengthOfOneWire[Coil1]+LengthOfOneWire[Coil2]+Length
OfOneWire[Coil3]+LengthOfOneWire[Coil4]+LengthOfOneWire[Coil
5]+LengthOfOneWire[Coil6]+LengthOfOneWire[Coil7]
 LengthOfAllWires[Coil1,Coil2,Coil3,Coil4,Coil5,Coil6,Coil7]
```
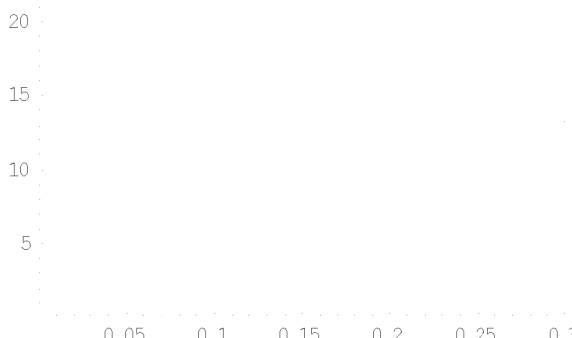176.656

Plotting B-field for each coil segment:
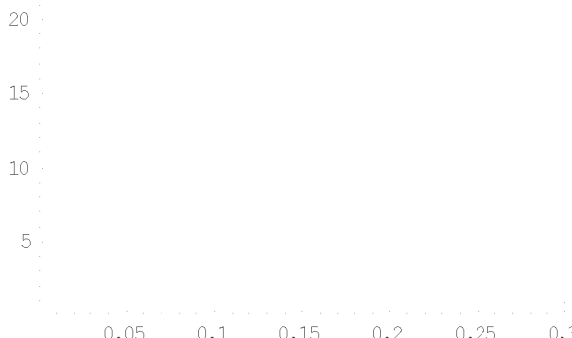
```
plotB8=Plot[B8[z],{z,0,.3}];
```

```
 FindMaximum[B8[z],{z,0}]
 {22.1329,{z→0.280169}}
```

```
plotB7=Plot[B7[z],{z,0,.3}];
```
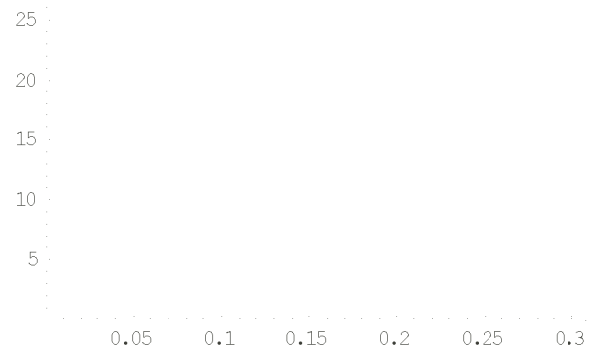
```
 FindMaximum[B7[z],{z,0}]
  {22.1329,{z→0.240069}}
```
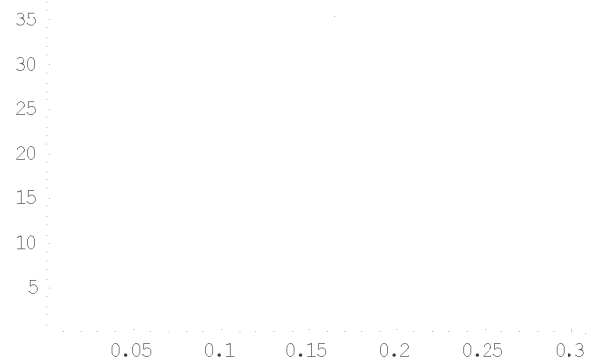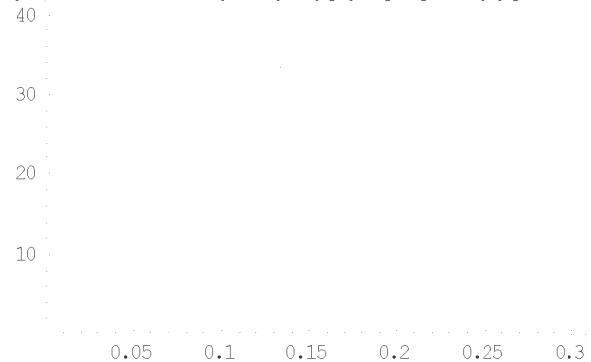
```
plotB6=Plot[B6[z],{z,0,.3}];
```



```
 FindMaximum[B6[z],{z,0}]
 {27.0928,{z→0.199969}}
```

```
plotB5=Plot[B5[z],{z,0,.3}];
```
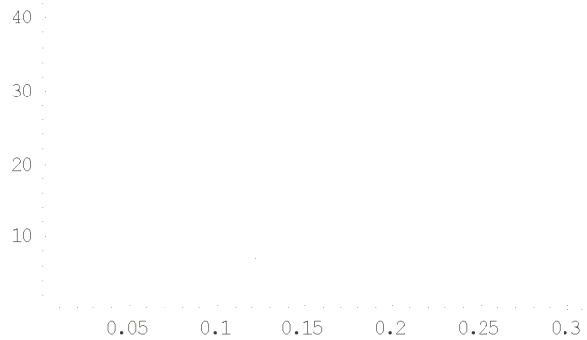


```
 FindMaximum[B5[z],{z,0}]
 {36.3988,{z→0.159869}}
```
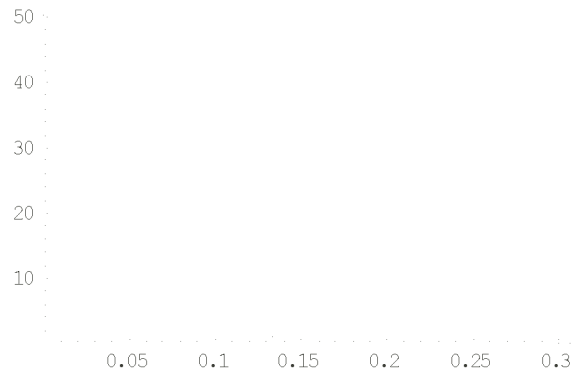
```
plotB4=Plot[B4[z],{z,0,.3}];
```



```
 FindMaximum[B4[z],{z,0}]
 {40.7677,{z→0.119769}}
```
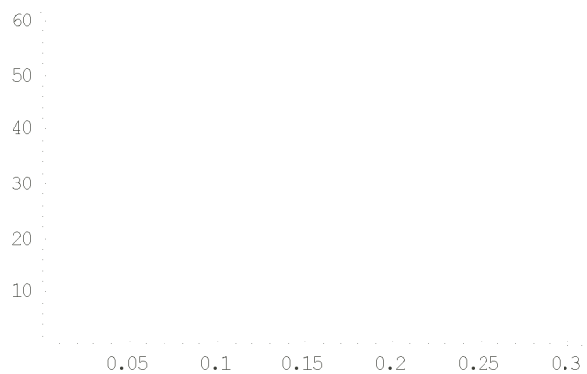
```
plotB3=Plot[B3[z],{z,0,.3}];
```



```
FindMaximum[B3[z],{z,0}]
{44.962,{z→0.079669}}
```

```
plotB2=Plot[B2[z],{z,0,.3}];
```



```
FindMaximum[B2[z],{z,0}]
{48.9921,{z→0.039569}}
```

```
plotB1=Plot[B1[z],{z,0,.3}];
```



```
FindMaximum[B1[z],{z,0}]
{60.1947,{z→-0.00053099}}
```

Appendix B

TurboCad Drawings

Qty.	A
1	0.75
2	1.00
2	1.25
3	1.50

Drill tap for 1/4 - 20
Depth 0.05in

1.51 in

0.75in

0.75 in   0.38in

A"

1/2A"

0.25 in

Drill and tap for #8-32
Depth 0.4 in

0.25 in

	TITLE			
		RETAINING BAR		
	SIZE	CAGE CODE	DWG NO	REV
Ingrid Kaldre	A			
	SCALE		SHEET	

$0.175 \begin{smallmatrix} +0.005 \\ 0.000 \end{smallmatrix}$ in

30°

Slots are identical. Bottom detail (round or flat)
unimportant

0.75 in

Ø5.0 in

Ø1.060 in

Material

0.050 in Copper Sheet

TITLE

Disk

Ingrid Kaldre

SIZE	CAGE CODE	DWG NO		REV
A				
SCALE			SHEET	

14.5 in

1.510 in   Note: Internal spacing should be the same for all disks   0.73 in   1.002 in

Turn and face
both ends of tube

0.970 in

Disk   Disk

Material	1in O.D. #304 SS Tube 10 Disk			
TITLE	**Slower Assembly**			
Ingrid Kaldre	SIZE **A**	CAGE CODE	DWG NO	REV
	SCALE		SHEET	

Bibliography

[1] Dr. David P. Stern. The solar wind. June 2004.

[2] Albert Einstein. On the quantum theory of radiation. *Phys Z.*, 18:121–128, 1917.

[3] William D. Phillips. Laser cooling and trapping of neutral atoms. *Rev. Mod. Phys.*, 70(3):721–738, July 1998.

[4] David J. Griffiths. *Introduction to Quantum Mechanics.* Prentice Hall, Inc., 1995.

[5] S. Tan Q. Chen, J. Stajic and K. Levin. Bcs-bec crossover: From high temperature superconductors to ultracold superfluids. *Physics Reports*, 412:1, 2005.

[6] Kenneth M. O'Hara. *Optical Trapping and Evaporative Cooling of Fermionic Atoms.* Physics, Duke University, 2000.

[7] Michael E. Gehm. *Preparation of an Optically-Trapped Degenerate Fermi Gas of ^6Li: Finding the Route to Degeneracy.* Physics, Duke University, 2003.

[8] Christopher A. Baird. Design and characterization of a multi-coil zeeman slower. Masters of arts in physics, Duke University, 1996.

[9] Margaret Harris. Design and construction of an improved zeeman slower. Undergraduate, Duke University, April 2003.

[10] MWS Wire Industries. Copper wire resistance values. March 2006.